Evaluation of Absorption and Emission Cross Sections of Er-Doped $LiNbO_3$ for Application to Integrated Optic Amplifiers

Chi-hung Huang, Leon McCaughan, *Member, IEEE*, and Douglas M. Gill

***Abstract*—The polarization-dependent absorption and emission spectra of the $^4I_{13/2}$–$^4I_{15/2}$ transition ($\lambda \sim 1.5$ μm) in single crystal bulk Er:$LiNbO_3$ have been measured. Low-temperature (10 K) measurements of the Stark split energy levels of these two manifolds indicate at least two Er^{3+} sites. McCumber theory is applied to determine the Er:$LiNbO_3$ absorption and emission cross sections. These values are used to calculate the gain characteristics of Er:$LiNbO_3$ channel waveguides. Calculations indicate that a gain of 10 dB is achievable in a waveguide of several centimeters using ~20-mW pump power.**

I. Introduction

RARE-EARTH doped materials have received renewed attention because of the availability of a broad range of diode laser pumps. Recent research interest has focused on Er-doped materials because the $^4I_{13/2} \rightarrow {}^4I_{15/2}$ transition of Er^{3+} emits at $\lambda = 1.5$ μm, a wavelength useful for fiber communications. The most notable achievement so far has been the Er-doped glass fiber [1]. Fiber lasers [2], [3] and traveling-wave amplifiers [4], [5] have been demonstrated and modeled [6], [7]. Recently, work has also begun on Er-doped Ti:$LiNbO_3$ waveguide devices. These devices have the potential for co-integration with other optical devices, such as optical switches and modulators. Stimulated emission [8] and laser operation [9] based on this material have been realized.

Unlike silica fiber, $LiNbO_3$ is a crystalline material. Er atoms in a $LiNbO_3$ host are likely to have well-defined lattice site locations, reducing the inhomogeneous broadening, and should therefore have better pumping and amplification efficiencies than Er-doped fibers. Er:$LiNbO_3$ devices demonstrated to date have been made with planar-doped substrates. Planar-doped or bulk-doped $LiNbO_3$, however, is not optimal for integrated optical circuits, in general, since it requires that the entire waveguide circuit be pumped to transparency. Equally restrictive, the transverse distribution of the active medium cannot be optimized. Recently, we have demonstrated a method for locally incorporating significant concentrations of Er^{3+} by way of co-diffusion with Ti [10] as an effort to provide a more flexible doping scheme.

In order to predict the gain of devices with a nonuniformly distributed active medium, a knowledge of the absorption and emission cross sections is essential. In this paper two methods of determining these cross sections are discussed. We have found the generally used Ladenburg–Fuchtbauer relationship [11], [12] to be inappropriate for this case. Instead, we apply McCumber theory [13] using the Stark split $^4I_{13/2}$ and $^4I_{15/2}$ energy levels measured from 10 K polarized absorption and emission spectra. Employing these cross sections (assuming that bulk-doped Er:$LiNbO_3$ yields the same cross section values as in locally doped waveguides), we calculate the gain characteristics, with consideration of the amplified spontaneous emission (ASE), of Er-doped $LiNbO_3$ channel waveguides by applying steady-state rate equations and simplified optical mode and Er^{3+} concentration profiles in the waveguides.

II. Theory

The optical gain of a medium is defined as

$$\gamma(\nu) = \frac{1}{I_\nu(z)} \frac{dI_\nu(z)}{dz} \tag{1}$$

where $I_\nu(z)$ is the light intensity at frequency ν along the z direction. If the gain is provided by the transition between two quantum states of the active material, then the gain coefficient can be written as

$$\gamma(\nu) = N_u \sigma_{\mathrm{em}}(\nu) - N_l \sigma_{\mathrm{ab}}(\nu) \tag{2}$$

where N_l, N_u, $\sigma_{\mathrm{em}}(\nu)$ and $\sigma_{\mathrm{ab}}(\nu)$ are the populations of the lower and upper energy states, and the emission and absorption cross sections, respectively. In order to predict the gain coefficient of a device with a nonuniformly distributed active medium, such as optical fibers or waveguides, it is first necessary to measure the material cross sections and then integrate the spatial overlap between the population profiles and the optical fields to obtain the effective gain of the structure.

We now consider the Er^{3+} $^4I_{13/2}$–$^4I_{15/2}$ transition as a three-level laser system. These two states are separated by an energy difference ($\Delta E \sim 0.8$ eV) which is large compared to $k_B T$ at or below room temperature. The population of the $^4I_{15/2}$ ground state can therefore be approximated by $N_l \cong N_o$

Manuscript received June 17, 1993; revised October 18, 1993. This work was supported in part by NSF under Grants ECS-9204852, and a Newport Research Award (to D. M. Gill).

C. Huang and L. McCaughan are with the Department of Electrical and Computer Engineering, University of Wisconsin–Madison, Madison, WI 53706, USA.

D. M. Gill is with the Material Science Program, University of Wisconsin–Madison, Madison, WI 53706, USA.

IEEE Log Number 9215934.

(the concentration of the active medium) when the material is not pumped. The absorption cross section

$$\sigma_{ab}(\nu) \cong -\gamma(\nu)/N_o \tag{3}$$

can be obtained by measuring the absorption coefficient $\alpha(\nu) = -\gamma(\nu)$ of the material.

A problem arises when determining the emission cross section, since in general it is difficult to determine N_u and N_l accurately when the material is being pumped. One option for measuring the cross sections is based on the Ladenburg–Fuchtbauer (L-F) relationship [11], [12] obtained from the basic Einstein transition equations [14]

$$\sigma_{ab}(\lambda) = A\frac{\lambda_{ab}^2}{8\pi n^2}\frac{g_u}{g_l}\frac{I_{ab}(\lambda)}{\int I_{ab}(\lambda)\frac{c}{\lambda^2}d\lambda} \tag{4}$$

$$\sigma_{em}(\lambda) = A\frac{\lambda_{em}^2}{8\pi n^2}\frac{I_{em}(\lambda)}{\int I_{em}(\lambda)\frac{c}{\lambda^2}d\lambda}. \tag{5}$$

Here n is the refractive index, λ_{ab} and λ_{em} are the peak wavelengths of these two spectra, and g_u and g_l are the degeneracies of the upper and lower states, respectively. A is the radiative transition rate of these two states, and is equal to $1/\tau$ (τ is the spontaneous emission lifetime) when no other process (nonradiative transition, etc.) takes place. The absorption and emission spectra $I_{ab}(\lambda)$ and $I_{em}(\lambda)$ can be measured on an arbitrary linear scale, and the integration is carried out over the whole spectrum of the transition.

The L-F relationship is an approximation based on two important assumptions: a) the material is isotropic, or at least the spectra along all polarization directions are taken to be identical [15]; and b) in the case where the states are comprised of a manifold of levels, the transition rates (A_{ul}) between any two levels (Fig. 1) are assumed to be equal [16]. As is shown below, neither of these two assumptions are appropriate for Er-doped $LiNbO_3$. Indeed, it has been found that L-F equation is not applicable for Er^{3+} in glass because of its temperature-dependent fluorescence lifetime [17]. To overcome the problems of the L-F theory for nonisotropic transitions between degenerate or near-degenerate states, McCumber [13] derived a relation to determine the emission cross section from the measured absorption cross section. Consider a transition between a specific level u in the upper manifold and a specific level l in the lower manifold. The absorption and emission cross sections for these two levels are taken to be equal, $\sigma_{lu}(\nu_{lu}) = \sigma_{ul}(\nu_{ul})$, so long as the measurements are made along a common optical propagation direction and polarization. (This is equivalent to $B_{12} = B_{21}$, the Einstein transition coefficients for a single-level-to-single-level transition.) Assuming that the state population within each manifold has a Boltzmann distribution profile (Fig. 1), the "effective" cross sections for the total transition between these two manifolds can be described as a summation of all the individual cross sections, with the Boltzmann population of the initial state as a weighting factor [18]

$$\sigma_{em}(\nu) = \frac{\Sigma_u\Sigma_l \exp(-E_u/k_BT)\sigma_{ul}(\nu)}{P_{upper}} \tag{6}$$

and

$$\sigma_{ab}(\nu) = \frac{\Sigma_l\Sigma_u \exp(-E_l/k_BT)\sigma_{lu}(\nu)}{P_{lower}} \tag{7}$$

where

$$P_{upper} = \Sigma_u \exp(-E_u/k_BT) \tag{8}$$

and

$$P_{lower} = \Sigma_l \exp(-E_l/k_BT) \tag{9}$$

are the partition functions for these two manifolds. If we multiply the numerator and the denominator of (6) by the common term $P_{lower}\exp[(E_{UL} - h\nu)/k_BT]$ (which is independent of the states u and l), (6) becomes

$$\sigma_{em}(\nu) = \frac{\Sigma_u\Sigma_l \exp[(-E_u - E_{UL} + h\nu)/k_BT]\sigma_{ul}(\nu)}{P_{lower}} \times \frac{P_{lower}}{P_{upper}} \exp[(E_{UL} - h\nu)/k_BT] \tag{10}$$

where E_{UL} is the energy separation between the lowest levels of the two manifolds. We can see from Fig. 1 that

$$h\nu - E_{UL} = E_u - E_l. \tag{11}$$

Substituting (11) and (7) into (10), and using

$$\sigma_{lu}(\nu) = \sigma_{ul}(\nu),$$

$\sigma_{em}(\nu)$ becomes

$$\sigma_{em}(\nu) = \sigma_{ab}(\nu)\frac{P_{lower}}{P_{upper}} \exp[(E_{UL} - h\nu)/k_BT]. \tag{12}$$

The partition functions P_{lower} and P_{upper} can be determined from (8) and (9) once the energy levels within these two manifolds are known. The emission cross section can then be obtained from the measured absorption cross section using (12). It should be noted that this formula is an exact expression only for cross sections which are comprised of $\sigma_{ul}(\nu)$ with δ-function lineshapes. If the lineshapes are homogeneously or inhomogeneously broadened, the exponential function in (12) will decrease the magnitude of the cross section at wavelengths shorter than the peak wavelength of each transition, and increase the magnitude at longer wavelengths. In our case, where the linewidth is less than 5 nm, worst case distortion caused by the finite linewidth is calculated to be less than 5%, and it is effectively zero at the peak wavelengths (in which we are most interested).

III. Experimental Results

A bulk-doped $LiNbO_3$ sample (from Tianjin University, China) with an Er concentration of 1.0 mol% Er^{3+} ($1.9 \times 10^{20}cm^{-3} \pm 2\%$ as confirmed by neutron activation analysis measurement) was optically pumped from the ground state to the $^4F_{9/2}$ manifold by a dye laser providing a pump wavelength of 655.7 nm. Fluorescence spectra of the $^4I_{13/2} - ^4I_{15/2}$ transition were measured by a 0.5-m grating spectrometer with a resolution of 2 Å. The lifetime was measured to be 4.3 ms using a 1.48-μm laser diode pump. Absorption spectra of the

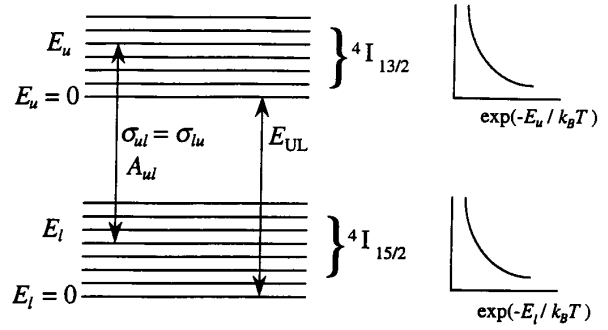

Fig. 1. The Stark split energy level diagram of Er^{3+} ions. There are 7 states in the $^4I_{13/2}$ manifold and 8 states in the $^4I_{15/2}$ manifold. In thermal equilibrium the state population in each manifold is described by Boltzmann distribution.

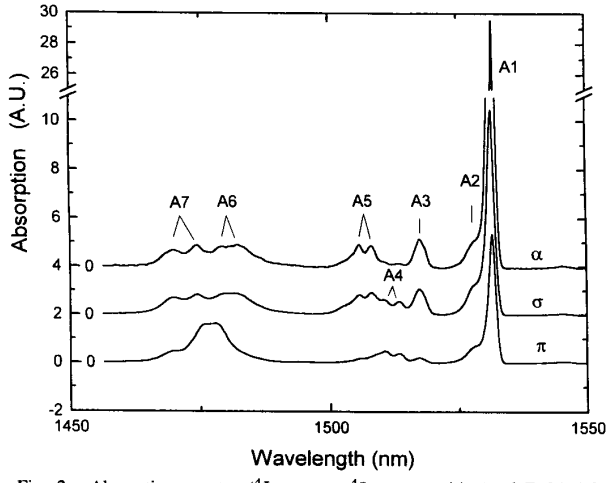

Fig. 2. Absorptions pectra ($^4I_{15/2} \rightarrow {}^4I_{13/2}$ transition) of Er:$LiNbO_3$ measured at 10 K. The exact wavelengths of these peaks can be found in Fig. 4.

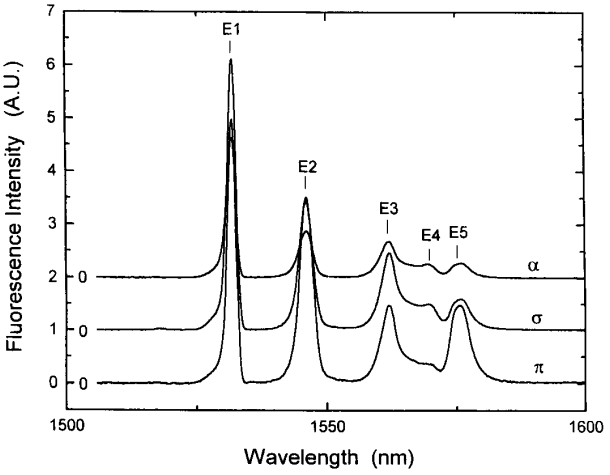

Fig. 3. Emission spectra ($^4I_{13/2} \rightarrow {}^4I_{15/2}$ transition) of Er:$LiNbO_3$ measured at 10 K. The exact wavelengths of these peaks can be found in Fig. 4.

sample were obtained using a monochromator with a broad-band tungsten–halogen light source. Spectra were measured both at 300 and 10 K. The 10 K absorption and emission measurements are used to identify the energy levels of both manifolds. At extremely low temperature the population in both manifolds essentially condenses to their respective lowest energy states, so the peak wavelengths of the fluorescence spectra represent the energy difference between the lowest state of the $^4I_{13/2}$ manifold and the multiple states in the $^4I_{15/2}$ manifold. Conversely, the 10 K absorption spectral peaks represent the energy difference between the lowest state of the $^4I_{15/2}$ manifold and the multiple states in the $^4I_{13/2}$ manifold.

The 10 K absorption and emission spectra along three different polarizations (α, σ, and π [15]) are shown in Figs. 2 and 3. Eight Stark split energy levels are found in the $^4I_{15/2}$ ground state as expected. (Three weak peaks not seen in Fig. 3 were measured from the $^4I_{11/2}$–$^4I_{15/2}$ emission spectra and indicated in Fig. 4.) In Fig. 2, however, we observe at least 11 peaks, more than the degeneracy (seven) of the $^4I_{13/2}$ manifold. The Er atoms therefore occupy more than one site in the $LiNbO_3$ crystal [19]. The absorption and emission transition lines corresponding to the assignments in Figs. 2 and 3 are illustrated in Fig. 4. For comparison, the Er^{3+} energy levels measured in other host materials as well as in $LiNbO_3$ are listed in Table I. Note that the measurements of $LiNbO_3$ by Gabrielyan [22] were made at 77 K and used unpolarized spectra. At this temperature the second lowest level of each manifold may be sufficiently populated to produce additional peaks, and the unpolarized thermally broadened spectra may leave some peaks unresolved.

From Figs. 2 and 3 we can see that the L-F relationship is not appropriate for this system because the absorption and emission spectra exhibit different lineshapes along different polarizations, meaning that the Er^{3+} ions are in an anisotropic environment. In addition, from the direct 300 K absorption measurements (Fig. 5, using (3)) we found that the peak cross sections derived from L-F relation (4) are 30–40% smaller than the measured values as shown in Table II.

McCumber theory is used, instead, to obtain the emission cross section from the measured absorption cross section (Fig. 5). Assuming, for simplicity, equal populations of two sites, the partition function ratio is calculated to be $P_{\text{lower}}/P_{\text{upper}} = 0.80$ at 300 K from the energy levels in Table I. (Note that if we consider only one site, the partition function ratio changes by less than 2%.) The derived emission cross sections at 300 K along the three polarization directions are shown in Fig. 6. The highest emission cross section value at 1531 nm is along the α polarization (2.25×10^{-20} cm^2), which means that a z-propagating waveguide on an x-cut $LiNbO_3$ substrate should have the largest optical gain. In this polarization the absorption cross section (and therefore the pumping efficiency) at 1485 nm has a relatively high value (0.5×10^{-20} cm^2). Note that the peak $\sigma_{\text{em}}(\nu)$ values along σ (TE) and π (TM) polarizations in a z-cut substrate is consistent with the lasing results at $\lambda =$ 1563 and 1576 nm reported in [23].

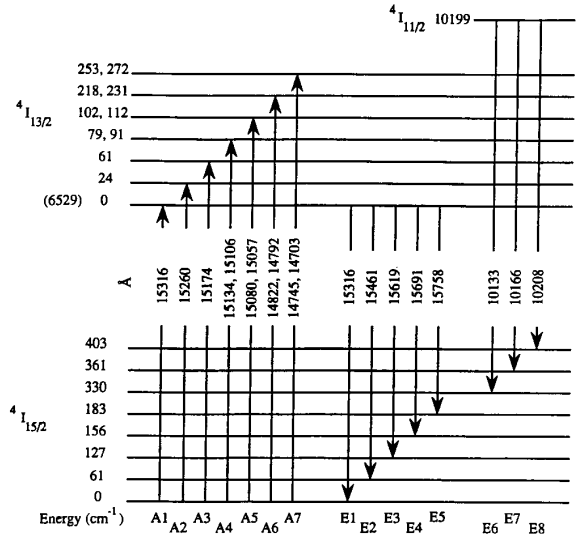

Fig. 4. The energy levels and the center wavelengths of the measured absorption and emission lines from Figs. 2 and 3.

TABLE I
STARK ENERGY LEVELS (in cm^{-1}) OF $^4I_{13/2}$ $-^4I_{15/2}$ MANIFOLDS OF Er^{3+} IONS MEASURED IN DIFFERENT HOST MATERIALS (Er_2O_3 [20], LaF_3 [21], $LiNbO_3$ [22], and this paper.)

	Er_2O_3		LaF_3		$LiNbO_3$ (77 K)		This Paper
$^4I_{13/2}$							
	357		220		254, 280		253, 272
	330		141		235		218, 231
	174		118		107		102, 112
	84		96		87		79, 91
	78		66		62		61
	32		24				24
(6510)	0	(6553)	0	(6524)	0	(6529)	0
$^4I_{15/2}$							
	505		443		414		403
	490		400		353		361
	265		314		278		330
	159		219		182		183
	88		200		156		156
	75		121		132		127
	38		51		63		61
	0		0		0		0

TABLE II
ABSORPTION CROSS SECTION PEAK VALUES AT 1531 nm OBTAINED FROM MEASUREMENT AND FROM LANDENBURG–FUCHTBAUER RELATIONSHIP ALONG THREE DIFFERENT POLARIZATIONS (The sample has an Er concentration of 1.9×10^{20} cm^{-3} and measured fluorescence lifetime of 4.3 ms.)

	σ_{ab}		
Polarization	Measured	L-F Equation	Difference
π	1.25×10^{-20}	0.88×10^{-20}	29.6%
σ	1.92×10^{-20}	1.14×10^{-20}	40.6%
α	2.75×10^{-20}	1.66×10^{-20}	39.6%

IV. GAIN CALCULATION OF $LiNbO_3$ CHANNEL WAVEGUIDES

We now calculate gain in a Ti-diffused waveguide which has been nonuniformly co-doped with Er. For an optical signal propagating in the z direction of a channel waveguide with

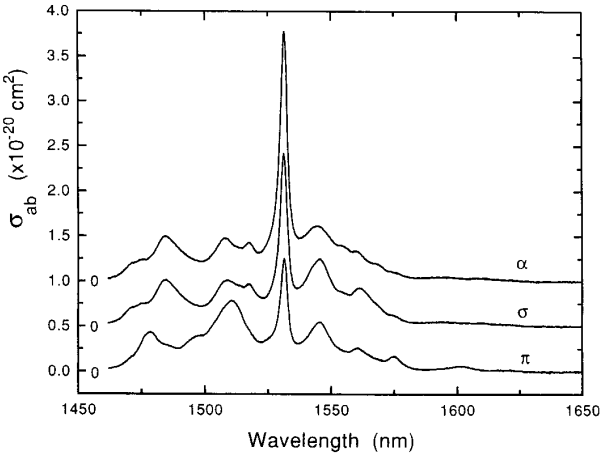

Fig. 5. Absorption cross section ($^4I_{15/2} \rightarrow {}^4I_{13/2}$ transition) of Er:$LiNbO_3$ measured at 300 K from bulk-doped crystals with 1.0 mol% Er^{3+} (1.9×10^{20} cm^{-3}). Cross section values are claculated from (3).

nonuniform active medium distribution, the gain equation can be written as an overlap integral

$$\frac{dP_{s,p}(z)}{dz} = \int_S P_{s,p}(z) f_{s,p}(x,y) \gamma_{s,p}(x,y,z)\, dx\, dy \qquad (13)$$

where $P_{s,p}(z)$ is the total signal or pump power in the waveguide's longitudinal direction z, and $f_{s,p}(x,y)$ is the optical intensity profile normalized over the waveguide cross section area, S, where

$$\int_S f_{s,p}(x,y)\, dx\, dy = 1.$$

To find the local gain coefficients for both signal and pump power, we use the steady-state rate equation for a three-level laser system

$$\frac{dN_u}{dt} = \sigma_{ab}(\nu_p)\frac{I_p}{h\nu_p}N_l - \frac{1}{\tau}N_u - [\sigma_{em}(\nu_s)N_u - \sigma_{ab}(\nu_s)N_l]\frac{I_s}{h\nu_s} \qquad (14)$$

where τ is the lifetime of the upper state, and

$$I_{s,p} = P_{s,p}(z) f_{s,p}(x,y)$$

are the local intensity of the signal and pump fields, respectively. (In this equation we ignore the stimulated emission induced by the pump field, and assume the pump state population relaxes to the upper state quickly compared to the lifetime of the upper state.) At local equilibrium, we have $dN_u/dt = 0$. Since the active medium concentration is just the sum of the ground state and upper state populations, $N_0 = N_l + N_u$, from (14) we get

$$N_u = \frac{\sigma_{ab}(\nu_p)\frac{I_p}{h\nu_p} + \sigma_{ab}(\nu_s)\frac{I_s}{h\nu_s}}{\sigma_{ab}(\nu_p)\frac{I_p}{h\nu_p} + [\sigma_{em}(\nu_s) + \sigma_{ab}(\nu_s)]\frac{I_s}{h\nu_s} + \frac{1}{\tau}} N_0 \qquad (15)$$

and

$$N_l = \frac{\sigma_{em}(\nu_s)\frac{I_s}{h\nu_s} + \frac{1}{\tau}}{\sigma_{ab}(\nu_p)\frac{I_p}{h\nu_p} + [\sigma_{em}(\nu_s) + \sigma_{ab}(\nu_s)]\frac{I_s}{h\nu_s} + \frac{1}{\tau}} N_0. \qquad (16)$$

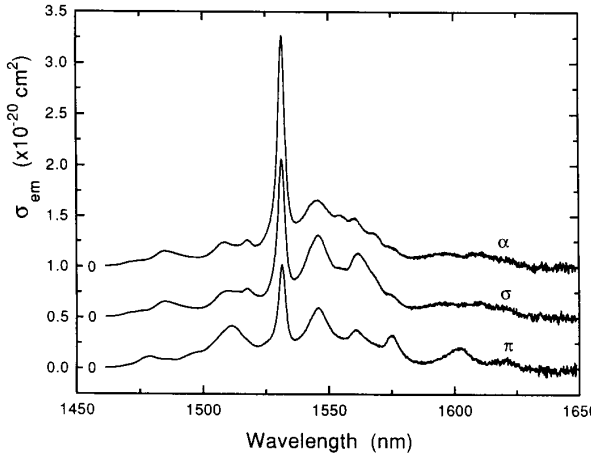

Fig. 6. Derived emission cross section ($^4I_{13/2} \rightarrow {}^4I_{15/2}$ transition) of Er:$LiNbO_3$ at 300 K.

The signal gain is given by

$$\gamma(\nu_s) = N_u\sigma_{\rm em}(\nu_s) - N_l\sigma_{\rm ab}(\nu_s) = \frac{\sigma_{\rm em}(\nu_s)\sigma_{\rm ab}(\nu_p)\frac{I_p}{h\nu_p} - \sigma_{\rm ab}(\nu_s)\frac{1}{\tau}}{\sigma_{\rm ab}(\nu_p)\frac{I_p}{h\nu_p} + [\sigma_{\rm em}(\nu_s) + \sigma_{\rm ab}(\nu_s)]\frac{I_s}{h\nu_s} + \frac{1}{\tau}}N_0, \tag{17}$$

and the pump power loss coefficient is

$$\alpha(\nu_p) = -\gamma(\nu_p) = \sigma_{\rm ab}(\nu_p)N_l = \frac{\sigma_{\rm ab}(\nu_p)\frac{1}{\tau} + \sigma_{\rm ab}(\nu_p)\sigma_{\rm em}(\nu_s)\frac{I_s}{h\nu_s}}{\sigma_{\rm ab}(\nu_p)\frac{I_p}{h\nu_p} + [\sigma_{\rm em}(\nu_s) + \sigma_{\rm ab}(\nu_s)]\frac{I_s}{h\nu_s} + \frac{1}{\tau}}N_0. \tag{18}$$

Note that amplified spontaneous emission (ASE) is not considered in the above derivation. At the gain region higher than 20 dB, however, ASE can significantly reduce the effective gain due to saturation. To take ASE into account, we can write the forward-traveling ($P^+_{\rm ASE}$) and the backward-traveling ($P^-_{\rm ASE}$) ASE signal as follows:

$$\frac{dP^{\pm}_{\rm ASE}(z)}{dz} = \int_S \{\pm P^{\pm}_{\rm ASE}(z)f_s(x,y)\gamma_s(x,y,z) \mp mP_0f_s(x,y)\sigma_{\rm em}(\nu_s)N_u(x,y,z)\}\,dx\,dy. \tag{19}$$

The second term in the integrand is attributed to the spontaneous emission power generated by the upper state population. m is the number of modes supported in the waveguide, which is 2 in a single-mode guide due to the two fundamental TE and TM modes. $P_0(= h\nu_s\Delta\nu_{\rm eff})$ is obtained from the effective linewidth ($\Delta\nu_{\rm eff}$) [6] of the emission lineshape to simplify the required calculation for the whole spontaneous emission spectrum. For α-polarization, $\Delta\nu_{\rm eff} = 2.5 \times 10^{12}$ Hz is calculated from Fig. 6 and used in our following calculation examples. Meanwhile, all the I_s terms in (14)–(18) must be replaced by $OI_s + I^+_{\rm ASE} + I^-_{\rm ASE}$ to take the saturation effect by ASE into account.

For a Ti-diffused waveguide, the fundamental mode of the optical intensity profile $f_{s,p}(x,y)$ can be modeled [24] by the equation

$$f_{s,p}(x,y) = C_1(y/D_I)^2\exp(-y^2/D_I^2)\exp(-x^2/W_I^2) \tag{20}$$

where C_1 is the normalization constant for $f_{s,p}$. W_I and D_I are the half-width and the full-depth constants of the intensity profile, respectively, which are determined from the diffusion conditions, material properties, and wavelength. Assuming an infinite Er source, the surface in-diffused Er concentration profile can be written [25] as

$$N_0(x,y) = C_2\exp(-y^2/D_N^2) \cdot \left\{\mathrm{erf}\left(\frac{W_N + 2x}{2D_N}\right) + \mathrm{erf}\left(\frac{W_N - 2x}{2D_N}\right)\right\}N_{\max} \tag{21}$$

where W_N is the width of the Er film before diffusion, and D_N is the $1/e$ depth after diffusion. C_2 is scaled so that the maximum of $N_0(x,y)$ is $N_{\max}$, which depends on the diffusibility and solubility of Er, and is at $(x,y) = (0,0)$ for surface in-diffusion. Using the values of $f_{s,p}(x,y), N_0(x,y)$, and the input signal and pump power at $z = 0$, together with the boundary conditions $P^+_{\rm ASE}(z = 0) = 0$ and $P^-_{\rm ASE}(z = L) = 0$ for ASE, we can numerically solve the coupled differential equations (13) and (19) to find the signal gain, pump power, and ASE at any distance z of the waveguide.

We use the following particular waveguide parameters for our calculations: signal wavelength = 1.531 μm, pump wavelength = 1.485 μm, $W_I = 4$ μm, and $D_I = 4$ μm for both signal and pump field, $W_N = 4$ μm, and $\tau = 4.3$ ms as measured from our sample. The crystallographic orientation is x-cut with z propagation, which has the best cross-section values as determined above. In the following graphs, the abscissa is plotted as a (Length) $\times$ ($N_{\max}$) product. Fig. 7 shows the effect of diffusion depth D_N on the small-signal gain with 20-mW pump power. We can see that uniformly doped waveguides provide the largest differential gain over short waveguide lengths. However, for a given amplifier length and pump power, maximizing the gain requires a careful choice of Er concentration profile. For longer lengths, a reasonable active medium distribution is the one that matches the optical intensity profile of the pump [7]. The dashed line in Fig. 7 shows the gain of such a speculative Er profile. We also found that (calculations not shown), because the lateral and vertical diffusion coefficients are approximately the same, the initial Er strip width (W_N) has little effect on the gain when the diffusion depth (D_N) is larger than the lateral optical mode size (W_I).

Fig. 8 shows the dependence of gain on pump power (using a diffused Er profile with $D_N = 4$ μm from [10]). Under these conditions the pump power required to reach transparency is 5 mW. A very reasonable gain performance can be achieved with 20–30-mW pump power. For example,

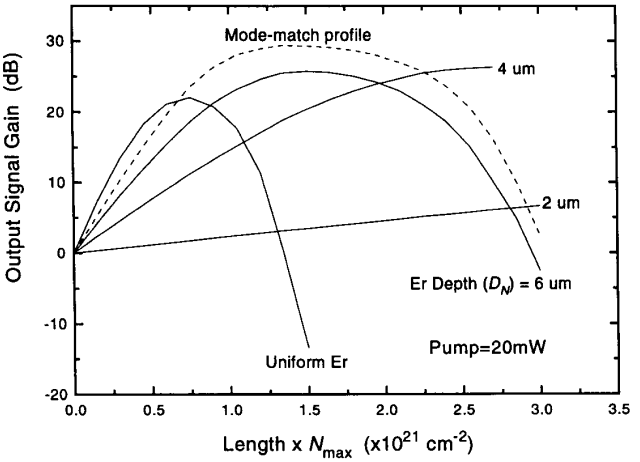

Fig. 7. Gain versus (Length) × ($N_{\max}$) product at several Er diffusion depths (D_N). The following conditions are used: $W_1 = 4$ μm, $D_1 = 4$ μm, $W_N = 4$ μm, and pump power = 20 mW. The dashed line has an Er profile the same as the pump optical field. The results for uniformly doped sample are also shown for comparison.

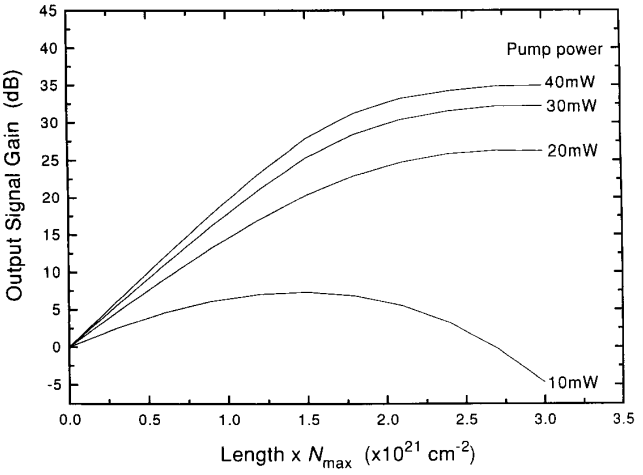

Fig. 8. Gain versus (Length) × ($N_{\max}$) product for several launched pump powers. $D_N = 4$ μm. W_I, D_I and W_N are all 4 μm as in Fig. 7.

using 20-mW pump power on a 3-cm-long waveguide with surface Er concentration of 1.9×10^{20} cm^{-3} (1.0 mol%) will produce 10-dB gain for y-polarized light in an x-cut substrate. For comparison, if we use x-polarized light in a z-cut substrate, the signal gain will be reduced to 6 dB. It should be noted that the gain coefficients are calculated for small input signal. For the previous conditions, an input signal power of 0.5 mW will saturate the output gain to half of its original value. Note that the gain saturation observed in Fig. 8 is due to ASE. For the (Length) × ($N_{\max}$) product used in our example (5.7×10^{20} cm^{-2}), the ASE power is 7 μW for 20-mW pump power.

We can estimate the pump–output relation of lasers based on this material by calculating the output ASE power with the boundary conditions that $P^{+}_{\mathrm{ASE}}(z=0) = R_1 P^{-}_{\mathrm{ASE}}(z=0)$ and $P^{-}_{\mathrm{ASE}}(z=L) = R_2 P^{+}_{\mathrm{ASE}}(z=L)$, where R_1 and R_2 are the mirror reflectances of the laser endfaces. Calculation shows that a threshold pump power ~10 mW and a slope efficiency 23% can be obtained for an Er:$LiNbO_3$ laser with 95% : 95% endface reflectances and a single-path pumping scheme, using (Length) × ($N_{\max}$) = 5.7×10^{20} cm^{-2}.

V. Conclusion

The energy levels of the $^4I_{13/2}$ and $^4I_{15/2}$ manifolds of single-crystal bulk Er:$LiNbO_3$ were obtained from low-temperature spectroscopy. At least two Er^{3+} sites appear to be present in the $LiNbO_3$ host. Absorption and emission cross sections along the various crystallographic axes were determined from McCumber theory. The peak emission cross section value (2.25×10^{-20} cm^2) of Er:$LiNbO_3$ at α polarization is about 3 times that of Er-doped fibers [17]. Not unexpectedly, the linewidth (~ 3 nm) is narrow compared to the ~ 10-nm width in silica fibers. With regard to pumping efficiency, the absorption cross section (0.5×10^{-20} cm^2) at

1485 nm is 2.5 times larger than that in a silica-glass host. Model calculations based on these results predict >10-dB gain can be achieved in a waveguide of several centimeters using 20 mW of pump power and moderate Er^{3+} concentration. It may therefore be possible to fabricate short, integrable, 1.5-μm optical amplifiers and lasers for Ti:$LiNbO_3$ integrated optics.

REFERENCES

[1] B. J. Ainalie, "A review of the fabrication and properties of erbium-doped fibers for optical amplifiers," *J. Lightwave Technol.* , vol. 9, no. 2, pp. 220–238, 1991.

[2] K. Iwatsuki, "Er-doped superfluorescent fiber laser pumped by 1.48 μm laser diode," *Photon. Technol. Lett.*, vol. 2, no. 4, pp. 237–238, 1990.

[3] L. Reekie, I. M. Jauncey, S. B. Poole, and D. N. Payne, "Diode-laser-pumped operation of an Er^{3+}-doped single-mode fibre laser," *Electron. Lett.* , vol. 23, no. 20, pp. 1076–1077, 1987.

[4] E. Desurvire, J. R. Simpson, and P. C. Becker, "High-gain erbium-doped traveling-wave fiber amplifier," *Opt. Lett.* , vol. 12, no. 11, pp. 888–890, 1987.

[5] T. Kashiwada, M. Shigenmatsu, T. Kougo, H. Kanamori, and Nishimura, "Erbium-doped fiber amplifier pumped at 1.48 μm with extremely high efficiency," *Photon. Technol. Lett.* , vol. 3, no. 8, pp. 721–723, 1991.

[6] C. R. Giles and E. Desurvire, "Modeling erbium-doped fiber amplifiers," *J. Lightwave Technol.*, vol. 9, no. 2, pp. 271–283, 1991.

[7] J. R. Armitage, "Three-level fiber laser amplifier: A theoretical model," *Appl. Opt.*, vol. 27, no. 23, pp. 4831–4836, 1988.

[8] S. Helmfrid, G. Arvidsson, J. Webjörn, M. Linnarsson, and T. Pihl, "Stimulated emission in Er:Ti:$LiNbO_3$ channel waveguides close to 1.53 μm transition," *Electron. Lett.* , vol. 27, no. 11, pp. 913–914, 1991.

[9] R. Brinkmann, W. Sohler, and H. Suche, "Continuous-wave erbium-diffused $LiNbO_3$ waveguide laser," *Electron. Lett.* , vol. 27, no. 5, pp. 415–417, 1991.

[10] D. M. Gill, A. Judy, L. McCaughan, and J. C. Wright, "Method for the local incorporation of Er into $LiNbO_3$ guided wave optic devices by Ti co-diffusion," *Appl. Phys. Lett.*, vol. 60, no. 9, pp. 1067–1069, 1992.

[11] J. N. Sandoe, P. H. Sarkies, and S. Parke, "Variation of Er^{3+} cross section for stimulated emission with glass composition," *J. Phys. D: Appl. Phys.* , vol. 5, pp. 1788–1799, 1972.

[12] R. R. Jacobs and M. J. Weber, "Induced-emission cross sections for the $^4F_{3/2} - {}^4I_{13/2}$ transition in neodymium laser glasses," *J. Quantum Electron.*, pp. 846–847, 1975.

[13] D. E. McCumber, "Einstein relations connecting broadband emission and absorption spectra," *Phys. Rev.*, vol. 136, no. 4A, pp. A954–A957, 1964.

[14] See, for example, J. T. Verdeyen,*Laser Electronics, 2nd ed. Englewood Cliffs, NJ: Prentice-Hall, 1989, ch. 7.*

[15] See, for example, B. Henderson and G. F. Imbusch, *Optical Spectroscopy of Inorganic Solids. Oxford, UK: Oxford Univ. Press, 1989, ch. 4.*

[16] E. Desurvire, "Study of the complex atomic susceptibility of erbium-doped fiber amplifiers," *J. Lightwave Technol.*, vol. 8, no. 10, pp. 1517–1527, 1990.

[17] W. L. Barnes, R. I. Laming, E. J. Tarbox, and P. R. Morkel, "Absorption and emission cross section of Er^{3+} doped silica fibers," *J. Quantum Electron.*, vol. 27, no. 4, pp. 1004–1009, 1991.

[18] S. S. Payne, L. L. Chase, L. K. Smith, W. L. Kway, and W. F. Krupke, "Infrared cross-section measurements for crystals doped with Er^{3+}, Tm^{3+} and Ho^{3+}," *J. Quantum Electron.* , vol. 28, no. 11, pp. 2619–2630, 1992.

[19] D. M. Gill, J. C. Wright, C. Huang, and L. McCaughan, manuscript in preparation.

[20] J. B. Gruber, J. R. Henderson, M. Muramoto, K. Rajnak, and J. Conway, "Energy levels of single-crystal erbium oxide," *J. Chem. Phys.*, vol. 45, no. 2, pp. 477–482, 1966.

[21] W. F. Krupke and J. B. Gruber, "Absorption and fluorescence spectra of Er^{3+} ($4f^{11}$) in LaF_3," *J. Chem. Phys.*, vol. 39, no. 4, pp. 1024–1029, 1963.

[22] V. T. Gabrielyan, A. A. Kaminskii, and L. Li, "Absorption and luminescence spectra and energy levels of Nd^{3+} and Er^{3+} ions in $LiNbO_3$ crystals," *Phys. Status Solidi A*, vol. 3, pp. K37–K41, 1970.

[23] P. Becker, R. Brinkmann, M. Dinand, W. Sohler, and H. Suche, "Er-diffused Ti:$LiNbO_3$ waveguide laser of 1536 and 1576 nm emission wavelengths," *Appl. Phys. Lett.*, vol. 61, no. 11, pp. 1257–1259, 1992.

[24] S. K. Korotky, W. J. Minford, L. L. Buhl, M. D. Divino, and R. C. Alferness, "Mode size and method for estimating the propagation constant of single-mode Ti:$LiNbO_3$ strip waveguides," *J. Quantum Electron.*, vol. 18, no. 10, pp. 1796–1801, 1991.

[25] G. B. Hocker and W. K. Burns, "Mode dispersion in diffused channel waveguides by the effective index method," *Appl. Opt.*, vol. 16, no. 1, pp. 113–118, 1977.

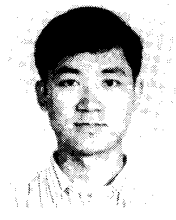

Chi-hung Huang was born in Taipei, Taiwan, on May 21, 1965. He received the B.S. degree in electronics engineering from the National Chiao-Tung University, Hsinchu, Taiwan, in 1987, and the M.S. degree in electrical engineering from the University of Wisconsin, Madison, in 1992.

He is currently working toward the Ph.D. degree at the University of Wisconsin, Madison. His research interests include the applications of nonlinear properties in integrated optics and fiber communications.

Leon McCaughan (M'84) received the M.S. degree in physics and the Ph.D. degree in biophysics from the University of Michigan, Ann Arbor.

From 1979 to 1980, he held a postdoctoral appointment with Brookhaven National Laboratory. From 1980 to 1984, he was with Bell Laboratories, where he was engaged in the research and development of integrated optic devices. He is currently a Professor in the Department of Electrical and Computer Engineering at the University of Wisconsin, Madison. His research includes guided wave integrated optics, nonlinear optics, and fiber optics.

Douglas M. Gill was born in Syracuse, NY, on September 5, 1962. He received the B.S. degree in physics from the State University of New York, College at Buffalo, in 1987, and the M.S. degree in material science from the University of Wisconsin-Madison, in 1989.

Currently, he is engaged in research towards the Ph.D. degree at the University of Wisconsin-Madison. His current research interests include the study of integrated optics with localized gain. He was the recipient of an OSA Newport fellowship.